HiSST: 3rd International Conference on High-Speed Vehicle Science Technology
14 -19 April 2024, Busan, Korea

Investigation on multi-channel gliding arc plasma enhanced supersonic ignition at near blowout limit

Tiangang Luo[1], Jiajian Zhu[2], Mingbo Sun[3], Yifu Tian[4]*, Minggang Wan[5], Yongchao Sun[6]*

Abstract

The ignition enhancement process of liquid kerosene at room temperature in a scramjet combustor by multi-channel gliding arc (MCGA) plasma was carried out under a Mach number of 2.5, a total temperature of 1600 K, and a total pressure of 1.65 MPa. The CH* images of the flame were synchronously captured by two high-speed cameras with a 20 kHz frame rate on the side and top of the combustor, and the schlieren images were captured on the side of the combustor with the same frame rate. The current and voltage waveforms of MCGA plasma discharge were simultaneously recorded with cameras. The flame kernel is formed at the discharge power peak of the MCGA plasma. The continuous discharge of MCGA plasma can generate multiple flame kernels. The merge of flame kernels contributes to the development of flame and the establishment of global flame. The ignition process of MCGA consists of three stages: flame kernel formation stage, flame propagation stage, and flame self-sustaining stage. MCGA plasma can provide repeatable enhanced ignition of kerosene within the GER range of 0.24 to 0.46. It can also maintain flame and enhance ignition near the lean blowout limit.

Keywords: *Gliding arc plasma, Scramjet, Blowout, Ignition enhancement, Flame propagation*

Nomenclature

MCGA – Multi-channel gliding arc
LEC – Leading edge of the cavity
TEC – Trailing edge of cavity
GER – Global equivalence ratio
APS – Adjustable power supply
DPO – Digital phosphor oscilloscope

1. Introduction

The airbreathing hypersonic vehicle can achieve ultra-fast and cost-effective round-trip and has broad application prospects in aerospace and other fields. The scramjet is the primary power device for airbreathing hypersonic vehicles. Problems such as engine flameout and re-ignition can occur during attitude adjustments and incoming flow condition changes of the vehicle [1]. Using a cavity flame holder can decrease the local flow speed, increase the residence time of the fuel, and significantly reduce the ignition delay time [2]. However, it is essential to note that the ability of the cavity flame holder to maintain the stability of the flame is still limited. After years of research and exploration, it has been found that plasma can realize the ignition of scramjet combustors. The plasma-enhanced ignition is based on three basic principles: thermal effect, kinetic effect, and transport effect [3]. Plasma can be classified as thermal or non-thermal equilibrium, depending on whether the plasma gas temperature is the same as the electron temperature. Gliding arc plasma is a non-equilibrium plasma that exhibits thermal and non-thermal equilibrium plasma characteristics. It has significant potential for achieving

[1] *National University of Defense Technology, China, luotiangang@nudt.edu.cn*
[2] *National University of Defense Technology, China, jjzhu@nudt.edu.cn*
[3] *National University of Defense Technology, China, sunmingbo@nudt.edu.cn*
[4] *National University of Defense Technology, China, tianyifu@nudt.edu.cn*
[5] *National University of Defense Technology, China, wanminggang18@nudt.edu.cn*
[6] *National University of Defense Technology, China, ycsun1989@163.com*

rapid ignition [4], reducing ignition delay time [5], improving combustion stability [6], and expanding the combustion boundary [7].

The Leonov team in Russia carried out extensive research on quasi-DC discharge and achieved enhanced ignition of ethylene fuel in supersonic airflow [8]. Ombrello et al. successfully achieved ignition of ethylene fuel in the scramjet combustor using spark discharge at Mach 2.0 [9]. Takita et al. developed a dual plasma jet igniter based on a scramjet combustor to achieve enhanced ignition of ethylene fuel at Mach 2.3 [10]. The process of laser-induced plasma ignition and spark discharge ignition of ethylene fuel at Mach 2.92 was investigated by An et al. [11]. The results indicate that the flame kernel formed by laser ignition increased faster than the spark ignition before reaching LEC and was almost the same in the rapid development stage. Feng et al. compared the process of ethylene ignition by a gliding arc and MCGA at Mach 2.92 [12]. The results show that using MCGA to enhance ignition compared to a gliding arc can reduce the flame propagation time by 48 % and shorten the ignition time by 61 %.

Although the ignition in supersonic flow using gliding arc plasma has been studied, there are few studies on the direct ignition of liquid kerosene fuel using MCGA plasma. In this paper, the ignition process of MCGA plasma under different GERs has been studied at Mach 2.5, a total temperature of 1600 K, and a total pressure of 1.65 MPa. The influence of MCGA on the ignition and flame propagation process of liquid kerosene with different GERs was studied using a current-voltage probe, high-speed photography, and high-speed Schlieren diagnostic methods. The process of MCGA enhanced ignition was revealed in this paper, which provides a reference for the subsequent study of ignition and stable combustion of liquid kerosene at near blowout limit.

2. Experimental setup and approach

The experiment was conducted at the National University of Defense Technology in a direct-connected test facility [13]. This test facility consists of an air heater, a Laval nozzle, a combustor, and a nozzle. The air heater burns a mixture of oxygen, air, and alcohol in specific proportions to create a high enthalpy flow at the combustor inlet. The combustor inlet flow conditions are Mach number 2.5, total temperature 1600 K, and total pressure 1.65 MPa. The structure of the combustor is displayed in Fig. 1. The inlet height of the combustor is 30 mm, and the width is 50 mm. The depth of the cavity is 10 mm, the length-to-depth ratio is 4, and the close-out ramp angle is 45°. The height difference between the LEC and TEC is 1 mm. The fuel injection position is 220 mm away from LEC, and a single hole with a diameter of 1 mm is used to spray liquid kerosene fuel perpendicular to the bottom wall. The MCGA plasma igniter is arranged at the bottom of the cavity, and the distance between the igniter and LEC is 25 mm. The combustor is equipped with removable quartz glass viewing windows on the top and side, with the top viewing window offering a width of 37 mm for observation purposes. The high-speed cameras record the ignition and flame propagation process in the combustor.

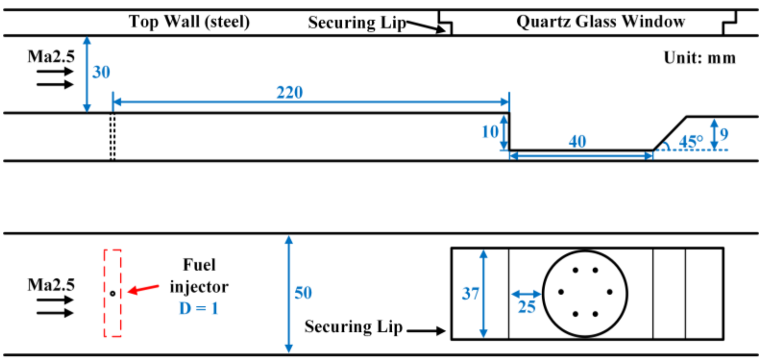

Fig. 1 The structure of the scramjet combustor

Three high-speed cameras were strategically positioned within the combustor to achieve real-time recording of the kerosene ignition process. The high-speed camera A (FASTCAM SA-X2) was placed on the side of the combustor, while the high-speed camera B (NAC Memrecam HX-7S) was suspended above it. Camera A had a 24 – 85mm zoom lens with f/5.6, while camera b had a 50 mm fixed-focus lens with f/2.8. The high-speed camera (FASTCAM SA-Z) was positioned on the side of the combustor, equipped with a 200 mm fixed-focus lens with f/4. Schlieren method was used to record the flow field changes during the ignition of kerosene enhanced by MCGA.

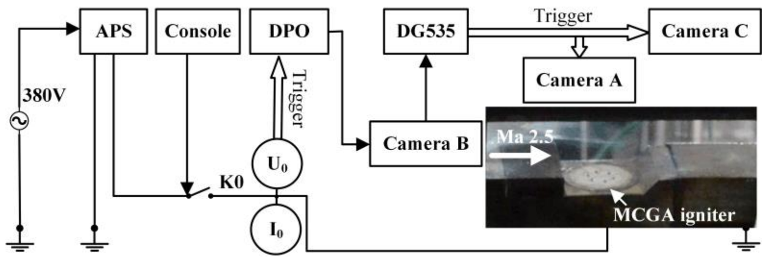

Fig. 2 The schematic diagram of the device position used in the experiment

The plasma adjustable power supply (CG-10000F)) has an input voltage of 380V and an output voltage of 340V during the experiment. The console regulates the switch of MCGA plasma. The DG535 synchronizes three cameras with a recording frequency of 20 kHz for the MCGA plasma discharge enhanced ignition. The digital phosphor oscilloscope (DPO-4054B) records the current (Pearson 6600), voltage (P6015A), and camera gates during the experiment. The experiment investigated the direct ignition of liquid kerosene using MCGA plasma discharge by varying the flow rate of kerosene injection. Table 1 presents the detailed experimental conditions, each repeated twice to thrice.

Table 1. Experimental conditions of kerosene with different GERs

Case	Mass flow rate (g/s)	GER	Ignition state
1	23.2	0.46	√
2	15.8	0.31	√
3	12.2	0.24	√
4	6.8	0.13	×

3. Results and discussion

3.1. MCGA plasma discharge characteristics

The discharge current and voltage waveforms of the ignition of MCGA plasma discharge at case 1 are shown in Fig. 3. Fig. 3(a) is the current and voltage waveforms of MCGA plasma discharge within 20 ms. During the ignition process, the average discharge power of MCGA plasma is 5456 W, the maximum peak voltage is 14 kV, and the maximum peak current is 9.2 A. Fig. 3(b) shows the partial amplification of MCGA plasma within 1 ms after the start of MCGA plasma discharge.

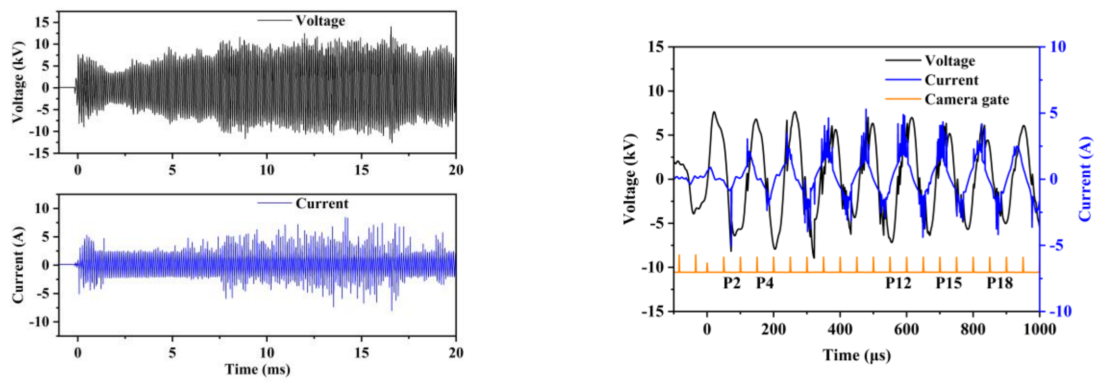

(a) MCGA plasma discharge within 20 ms. (b) MCGA plasma discharge within 1 ms.

Fig. 3 The waveforms of MCGA plasma discharge during ignition in case 1.

During the ignition process of MCGA (0 – 1 ms), many current spikes appear in the current waveform, and the discharge mode at this time corresponds to the spark type [14]. The instantaneous power of the spark discharge is high, which plays an important role in enhancing the ignition of liquid kerosene at room temperature. Fig. 3(b) shows the gate signal of the high-speed camera, which is used to combine the current and voltage of the MCGA discharge with the instantaneous image recorded by the high-speed cameras. The process of enhanced ignition of liquid kerosene by MCGA plasma is further analyzed in detail through the synchronization of discharge waveforms and images.

3.2. MCGA plasma ignition process

The MCGA plasma ignition process in case 1 is shown in Fig. 4. At the start of the MCGA plasma discharge of 50 μs, corresponding to P2 in Fig. 3(b), a significant current spike occurs in the camera gate, as shown in the current-voltage waveforms. Simultaneously, this event is accompanied by the generation of an arc, vividly captured from both the top and side views. At 150 μs, a flame kernel has formed around the MCGA plasma. This period coincides with observations from the schlieren image, which shows a significant accumulation of hot gas in the recirculation region near the LEC. At 700 μs (Fig. 4(a)-P15), MCGA plasma is observed from the top and side of the combustor, and the flame kernels attached to the MCGA plasma merge to form a larger flame. At the same time, it is observed from the side of the combustor that the flame kernel leaves the MCGA under the action of the recirculation zone in the cavity, and an initial flame is formed near the recirculation zone at LEC.

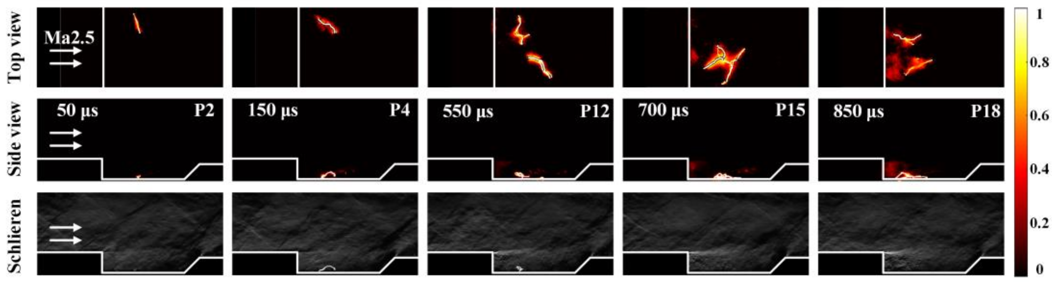

(a) MCGA plasma ignition process in 50–850 μs.

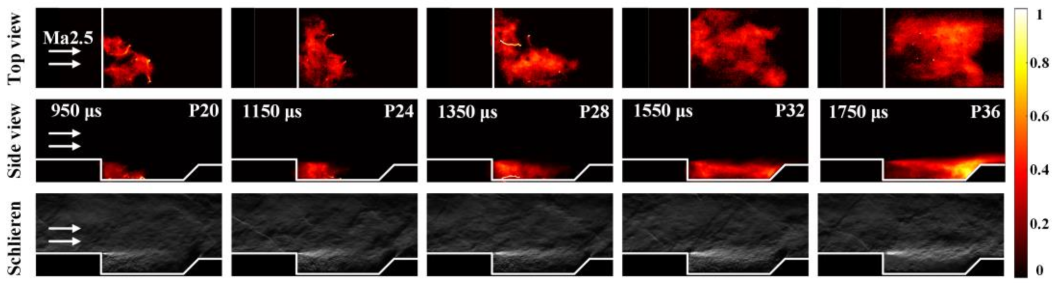

(b) MCGA plasma ignition process in 950–1750 μs.

Fig. 4 Instantaneous flame CH* chemiluminescence images are taken from the top and side of the combustor, and Schlieren images correspond to the side of the combustor in case 1.

At 850 μs (Fig. 4(a)-P18), MCGA forms the new flame kernel, and multiple flame kernels merge with the previous initial flame to form a large flame. At 950 μs (Fig. 4(b)-P20), after the initial flame was observed from the top to the front wall of the cavity, it began to rise under the action of the recirculation zone on both sides of the cavity and developed to both sides of the combustor. At 1150 μs (Fig. 4(b)-P24), the flame fills the cavity in the spanwise direction, and after lifting to the shear layer, it begins to develop towards the TEC. Due to the continuous discharge of MCGA plasma, new flame kernels and flames continue to merge (Fig. 4(b)-P28). At 1750 μs, the flame fills the cavity and establishes a global flame.

3.3. Enhanced ignition near the blowout limit with MCGA plasma

To study the influence of the change of GER on the direct ignition process of liquid kerosene fuel by MCGA plasma, the flame area in the instantaneous image of flame recorded from the side of the combustor is statistically and normalized. The normalized processing divides the instantaneous flame area by the maximum flame area, as shown in Fig. 5, and the ordinate unit is arbitrary (a.u.). According to the change of flame area, taking case 3 as an example, the ignition process is divided into three stages: flame kernel formation stage, flame propagation stage, and flame self-sustaining stage.

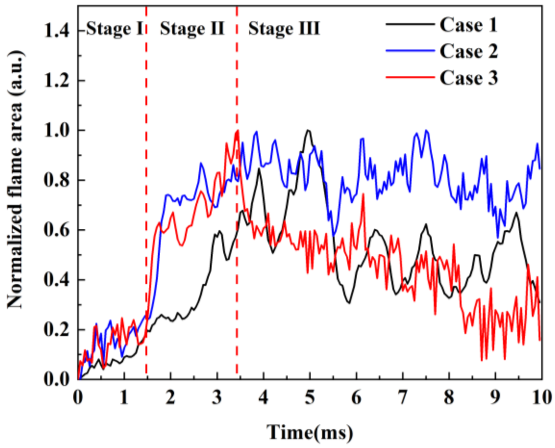

Fig. 5 The normalized flame area changes over time with different cases.

In the first stage (0 – 1.5 ms), the flame area is always less than 0.25 and oscillates. This is due to the continuous formation of flame kernels by MCGA discharge. The flame kernels continuously blowout under airflow, making it difficult to maintain stability and development. In the second stage (1.5 – 3.4 ms), under the continuous discharge of MCGA, the flame kernel is continuously blowout and continuously generated. The combustion products and heat converge near LEC under the action of the recirculation zone in the cavity to form a suitable ignition environment. Finally, a stable resident flame is formed and further developed until the maximum flame area is reached. In the third stage, the flame area decreases due to the blowout of partial flames. The above three stages exist in the ignition process of liquid kerosene with different GERs.

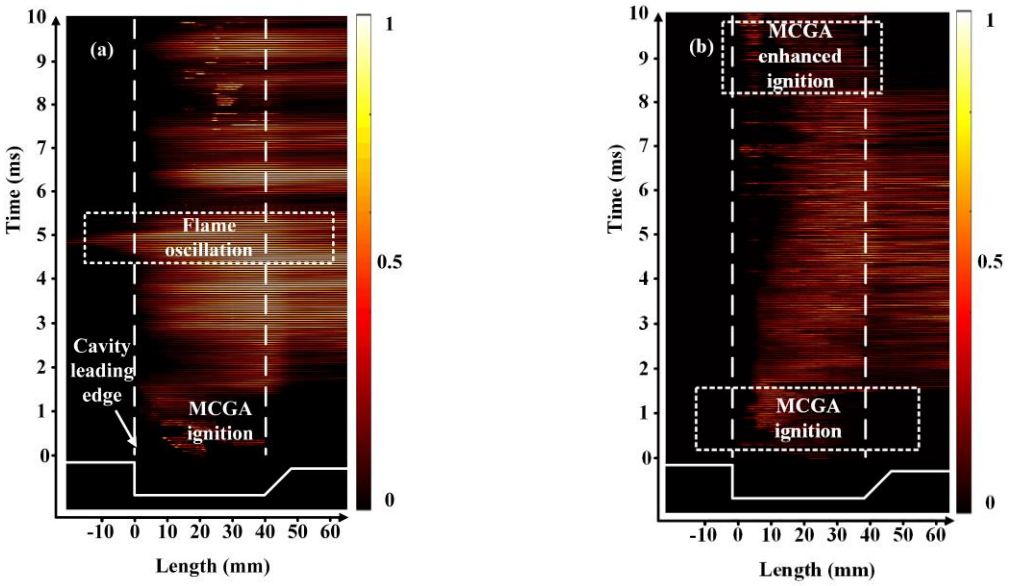

(a) Flame propagation trajectory in case 1. (b) Flame propagation trajectory in case 3.

Fig. 6 Flame propagation trajectories in the streamwise direction in different cases.

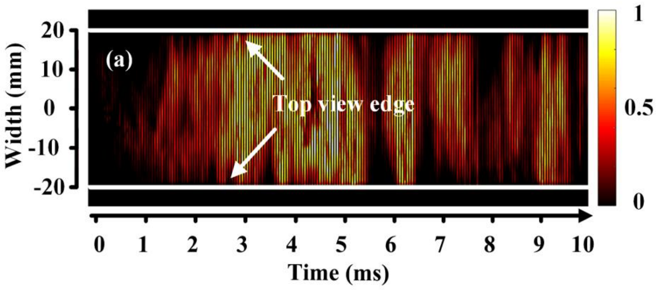

(a) Flame propagation trajectory in case 1.

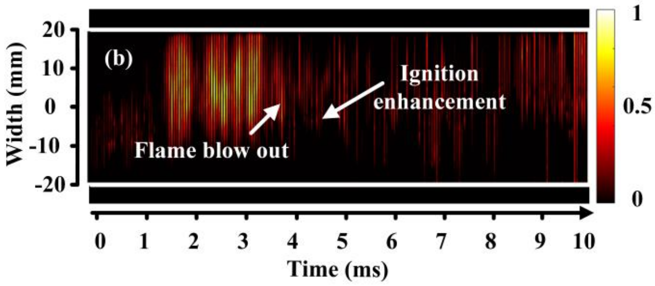

(b) Flame propagation trajectory in case 3.

Fig. 7 Flame propagation trajectories in the spanwise direction in different cases.

To further study the flame development process during MCGA ignition, the instantaneous images of a single flame recorded from the side of the combustor are accumulated along the vertical direction, and multiple images are accumulated along the vertical direction in chronological order. Fig. 6 and Fig. 7 are the integral diagrams of the streamwise and spanwise of the combustor in different cases. In case 1, from Fig. 6(a), it can be seen that the recirculation zone first influences the flame in the streamwise direction in the cavity to LEC, then develops to TEC until it fills the whole cavity. The flame crosses the LEC at about 5 ms, and the flame oscillation occurs. It can be seen from Fig. 7(a) that the flame is generated near the center axis of the combustor in the spanwise direction and then develops toward the walls on both sides of the combustor. In case 3, due to the lower GER, as shown in Fig. 6(b), the time to establish a global flame also gradually increases, and the flame propagation trajectory is similar to that of case 1, but the flame is extinguished and reignited within 8 – 10 ms.

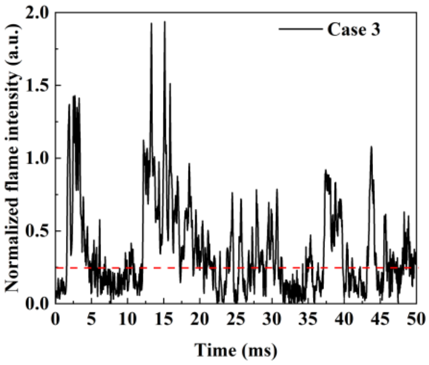

(a) Normalized flame intensity in case 3.

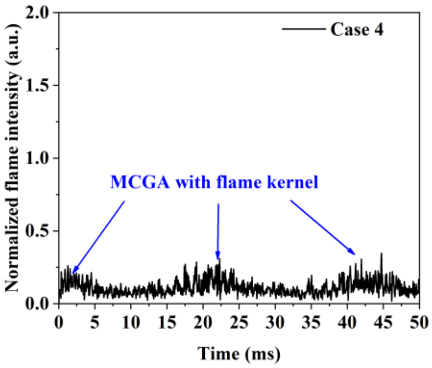

(b) Normalized flame intensity in case 4.

Fig. 8 The normalized flame intensity in streamwise direction changes with time in different cases.

To further study the enhanced ignition process of MCGA plasma on the combustion in near blowout conditions, Fig. 8(a) shows the development of normalized flame intensity with time in case 3. The normalization method divides the CH* intensity value of the flame in a single image by the average intensity value of the flame in the self-sustaining stage. It is difficult to maintain stable combustion for a long time, and blowout and re-ignition occur frequently. According to the normalized flame intensity value, the normalized flame intensity is divided into two regions: flame self-sustaining region and MCGA enhanced ignition region. The region where the normalized intensity value of the flame is above 0.25 is defined as the flame self-sustaining region. Although the flame intensity oscillates significantly in this region, there is no global extinction. The region where the normalized flame intensity value of the flame is below 0.25 is defined as the MCGA enhanced ignition region, where the flame is near to blowout or completely blowout. Fig. 8 (b) shows the development of normalized flame intensity with time in case 4. There are many spikes where the flame intensity is below 0.25 due to the continuous discharge of the MCGA plasma and the continuous flame generation near the MCGA plasma.

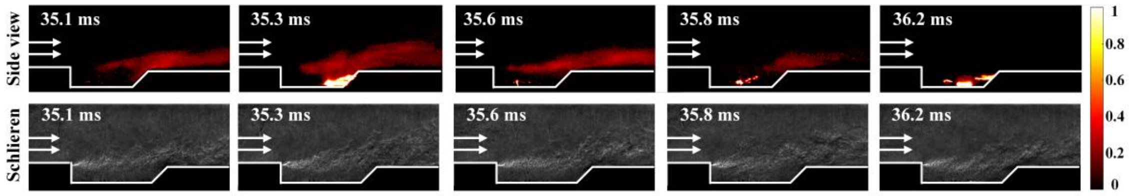

(a) Flame blowout process

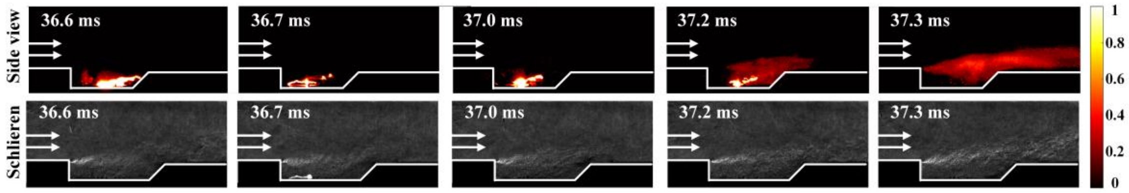

(b) MCGA enhanced ignition process

Fig. 9 MCGA re-ignition process after the flame blowout in case 3.

The instantaneous flame CH * chemiluminescence images and the schlieren images corresponding to Fig. 8 are shown in Fig. 9. The flame was completely extinguished at 36.2 ms. Flame kernel formation could still be observed around the MCGA plasma, and the generated flame kernels merged to form the initial flame. The global flame was re-established at 37.3 ms. Due to the continuous generation of the flame kernel by the MCGA plasma discharge, heat and products are continuously generated and accumulated [15]. This allows the flame to be maintained and re-ignition effectively achieved even after the flame has been extinguished. It is shown that the MCGA plasma has a repeatable enhanced ignition and a certain maintenance effect on the flame.

4. Summary and conclusions

In this paper, the experimental study of the direct ignition process of liquid kerosene by MCGA was carried out under the condition of Mach 2.5 and a total temperature of 1600 K in the combustor of a cavity-based scramjet. The influence of MCGA on the ignition and flame propagation process of liquid kerosene with different GERs was studied using a current-voltage probe, high-speed photography, and high-speed Schlieren diagnostic methods. The main conclusions are as follows:

(1) During the ignition process of MCGA, the flame kernel is generated with the MCGA plasma discharge at the power peak of the spark type discharge, and the flame kernels merge to form the initial flame. Under the effect of the cavity recirculation zone, the initial flame develops near the LEC and begins to develop on both sides. At the same time, it lifts into the shear layer and then develops to TEC until the global flame is established.

(2) There are three stages in the ignition process of liquid kerosene under supersonic flow by MCGA plasma: flame kernel formation stage, flame propagation stage, and flame self-sustaining stage. The main difference in the MCGA plasma ignition process under different GERs is the time difference between the flame kernel formation stage and the flame propagation stage.

(3) MCGA plasma can achieve repeatable enhanced ignition in the range of GER 0.24 to 0.46 of liquid kerosene. Under the near lean blowout limit, the continuous discharge of MCGA plasma requires certain maintenance on the flame.

Acknowledgments

This work is supported by the National Natural Science Foundation of China (NSFC) (Nos. 12322211, 12172379, and 11925207) and the Youth Independent Innovation Science Found Project of the National University of Defense Technology (No. ZK23-40).

References

1. Nakaya, S., Y. Hikichi, Y. Nakazawa, K. Sakaki, M. Choi, M. Tsue, M. Kono, S. Tomioka. Ignition and supersonic combustion behavior of liquid ethanol in a scramjet model combustor with cavity flame holder, Proc. Combust. Inst. 35, 2091-2099 (2015).
2. Ben Yakar, A., R.K. Hanson. Cavity Flame-Holders for Ignition and Flame Stabilization in Scramjets: An Overview, J Propul Power. 17, 869-877 (2001).
3. Ju Y, S. W.: Plasma assisted combustion: Dynamics and chemistry, Prog. Energy Combust. Sci. 21-83 (2015).
4. Feng, R., Y. Huang, J. Zhu, Z. Wang, M. Sun, H. Wang, Z. Cai. Ignition and combustion enhancement in a cavity-based supersonic combustor by a multi-channel gliding arc plasma, Exp. Therm Fluid Sci. 120, 110248 (2021).
5. Zhong, H., X. Mao, A.C. Rousso, C.L. Patrick, C. Yan, W. Xu, Q. Chen, G. Wysocki, Y. Ju. Kinetic study of plasma-assisted n-dodecane/O2/N2 pyrolysis and oxidation in a nanosecond-pulsed discharge, Proc. Combust. Inst. 38, 6521-6531 (2021).
6. Tian, Y., J. Zhu, M. Sun, H. Wang, Y. Huang, R. Feng, B. Yan, Y. Sun, Z. Cai. Enhancement of blowout limit in a Mach 2.92 cavity-based scramjet combustor by a gliding arc discharge, Proc. Combust. Inst. 39, 5697-5705 (2023).
7. Tang, Y., J. Sun, B. Shi, S. Li, Q. Yao. Extension of flammability and stability limits of swirling premixed flames by AC powered gliding arc discharges, Combust. Flame. 231, 111483 (2021).
8. Leonov SB, Y. DA.: Plasma-induced ignition and plasma-assisted combustion in high-speed flow, Plasma Sources Sci. Technol. 16, 132 (2007).
9. Hammack, S.D., T.M. Ombrello. Spatio-temporal evolution of cavity ignition in supersonic flow, Proc. Combust. Inst. Vol.38, 3845-3852 (2021).
10. Takita, K., K. Murakami, H. Nakane, G. Masuya. A novel design of a plasma jet torch igniter in a scramjet combustor, Proc. Combust. Inst. 30, 2843-2849 (2005).
11. An, B., L. Yang, Z. Wang, X. Li, M. Sun, J. Zhu, W. Yan. Characteristics of laser ignition and spark discharge ignition in a cavity-based supersonic combustor, Combust. Flame. 212, 177-188 (2020).
12. Feng R, Huang YH, Zhu JJ, Wang ZG, Sun MB, Wang HB, Cai Z. Ignition and combustion enhancement in a cavity-based supersonic combustor by a multi-channel gliding arc plasma, Exp. Therm Fluid Sci. 120, 110248 (2021).
13. Feng R, Wang ZG, Sun MB, Wang HB, Huang YH, Yang YX, Liu X, Wang C, Tian YF, Luo TG, Zhu JJ. Multi-channel gliding arc plasma-assisted ignition in a kerosene-fueled model scramjet engine, Aerosp. Sci. Technol. 126, 107606 (2022).
14. Zhu, J., J. Gao, A. Ehn, M. Aldén, Y. Kusano, Z. Li. Spatiotemporally resolved characteristics of a gliding arc discharge in a turbulent air flow at atmospheric pressure, Phys. Plasma. 24, 013514 (2017).
15. Luo, T., J. Zhu, M. Sun, R. Feng, Y. Tian, Q. Li, M. Wan, Y. Sun. MCGA-assisted ignition process and flame propagation of a scramjet at Mach 2.0, Chin. J. Aeronaut. 36, 378-387 (2023).

